

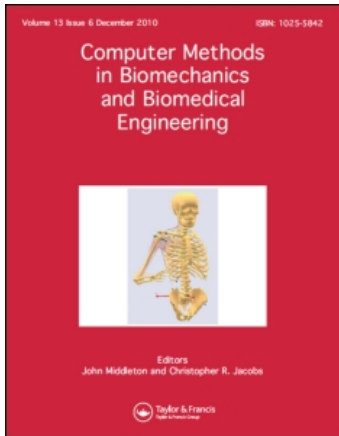
This article was downloaded by: [Bae, Ji Yong]

On: 27 January 2011

Access details: Access Details: [subscription number 932817475]

Publisher Taylor & Francis

Informa Ltd Registered in England and Wales Registered Number: 1072954 Registered office: Mortimer House, 37-41 Mortimer Street, London W1T 3JH, UK



Computer Methods in Biomechanics and Biomedical Engineering

Publication details, including instructions for authors and subscription information:

<http://www.informaworld.com/smpp/title~content=t713455284>

The biomechanical effect of the collar of a femoral stem on total hip arthroplasty

Insu Jeon^a; Ji-Yong Bae^a; Jin-Hong Park^a; Taek-Rim Yoon^b; Mitsugu Todo^c; Masaaki Mawatari^d; Takao Hotokebuchi^d

^a School of Mechanical Systems Engineering, Chonnam National University, Buk-gu, Gwangju, Republic of Korea ^b The Center for Joint Disease, Hwasun Hospital, Chonnam National University, Hwasun-Eup, Hwasun-Gun, Jeonnam, Republic of Korea ^c Research Institute for Applied Mechanics, Kyushu University, Kasuga, Fukuoka, Japan ^d Department of Orthopaedic Surgery, Saga University, Saga-City, Saga, Japan

Online publication date: 24 January 2011

To cite this Article Jeon, Insu , Bae, Ji-Yong , Park, Jin-Hong , Yoon, Taek-Rim , Todo, Mitsugu , Mawatari, Masaaki and Hotokebuchi, Takao(2011) 'The biomechanical effect of the collar of a femoral stem on total hip arthroplasty', Computer Methods in Biomechanics and Biomedical Engineering, 14: 1, 103 – 112

To link to this Article: DOI: 10.1080/10255842.2010.493513

URL: <http://dx.doi.org/10.1080/10255842.2010.493513>

PLEASE SCROLL DOWN FOR ARTICLE

Full terms and conditions of use: <http://www.informaworld.com/terms-and-conditions-of-access.pdf>

This article may be used for research, teaching and private study purposes. Any substantial or systematic reproduction, re-distribution, re-selling, loan or sub-licensing, systematic supply or distribution in any form to anyone is expressly forbidden.

The publisher does not give any warranty express or implied or make any representation that the contents will be complete or accurate or up to date. The accuracy of any instructions, formulae and drug doses should be independently verified with primary sources. The publisher shall not be liable for any loss, actions, claims, proceedings, demand or costs or damages whatsoever or howsoever caused arising directly or indirectly in connection with or arising out of the use of this material.

The biomechanical effect of the collar of a femoral stem on total hip arthroplasty

Insu Jeon^{a*}, Ji-Yong Bae^a, Jin-Hong Park^a, Taek-Rim Yoon^{b1}, Mitsugu Todo^{c2}, Masaaki Mawatari^d and Takao Hotokebuchi^d

^aSchool of Mechanical Systems Engineering, Chonnam National University, 300 Yongbong-dong, Buk-gu, Gwangju 500-757, Republic of Korea; ^bThe Center for Joint Disease, Hwasun Hospital, Chonnam National University, 160 Ilsimri, Hwasun-Eup, Hwasun-Gun, Jeonnam 519-809, Republic of Korea; ^cResearch Institute for Applied Mechanics, Kyushu University, 6-1 Kasuga-koen, Kasuga, Fukuoka 816-8580, Japan; ^dDepartment of Orthopaedic Surgery, Saga University, 5-5-1 Nabeshima, Saga-City, Saga 849-8501, Japan

(Received 20 October 2009; final version received 12 May 2010)

To investigate the biomechanical effect of collars, finite element analyses are carried out through two hip joints that are implanted using collared and collarless stems, respectively, and an intact hip joint model. For the analyses, the sacrum, coxal bone, and the cancellous and cortical bones of a femur are modelled using finite elements based on X-ray computed tomographic images taken from a 27-year-old woman. From the results, it is found that a collar with perfect calcar contact prevents stem subsidence and decreases the proximal–lateral gap and the lateral stem tilting. Therefore, it can impart reasonable biomechanical stability for total hip arthroplasty. However, its low load transmission ability and increased stem tilting effect due to the imperfect contact between the collar and the calcar are found to be serious problems that need to be solved. Results of clinical follow-up are presented for supporting the computational results.

Keywords: cementless collared stem; stem subsidence; proximal–lateral gap; stem tilting; calcar resorption; femoral fracture

1. Introduction

A collar is a projection on a femoral stem, which contacts with the resected neck of the proximal medial femur, called calcar, after total hip arthroplasty (THA). A designed, collared stem is introduced in cemented and cementless THA to solve the problems of collarless stems, such as the stress shielding effect and the subsidence of the stem into the femur (Eldridge et al. 1997; Loudon and Charnely 1980). However, there is still considerable controversy about the advantages and disadvantages of collared stems (Kwong 1990; Meding et al. 1999; Abdul Kadir et al. 2008). Generally, it is reported that the advantages of collared stems are (a) the prevention of stem subsidence and (b) an increase in the axial load transmission to the calcar when adequate contact is achieved between the collar and the calcar (Whiteside et al. 1988; Kelley et al. 1993). However, the reported disadvantage of collared stems is that during THA, it is difficult to obtain perfect contact between the collar and the calcar, which impairs the perfect transmission of the applied load to the femur (Fagan and Lee 1986). Though perfect contact can be achieved between the collar and the calcar, it is reported that the transmitted axial stress is still smaller than the normal stress level of the femur that is required for avoiding the stress shielding effect (Fagan and

Lee 1986). Furthermore, it has been reported that the varus deformation of the hip joint arises under a collared stem (Fagan and Lee 1986). Some long-term clinical follow-up results show that the presence of a collar has no effect on proximal femoral osteopenia (Carlsson et al. 1995; Meding et al. 1999).

In reality, to overcome the disadvantages of collared stems, a clear understanding of the biomechanical effect of collars on THA is necessary. In this research, we analyse comprehensively the biomechanical effects of collars using computational results and clinical follow-up data. As cemented femoral prostheses have been replaced by cementless prostheses recently to prevent the aseptic loosening of prostheses (Namba et al. 1998; Goetzen et al. 2005), an uncemented prosthesis is selected for this research. Finite element models of two hip joints that are implanted using collared and collarless stems, respectively, and an intact hip joint are constructed and used for the analysis. The von Mises stresses obtained from the models are compared with each other for evaluating the load-transmit efficiency of collars. Furthermore, the stem subsidence, the lateral and anterior tilting of the stem and the proximal–lateral gap between the stem and the cancellous bone, which cause stem micromotion and loosening and can be major causes of femoral fracture, are analysed.

*Corresponding author. Email: i_jeon@chonnam.ac.kr

2. Methods

2.1 3D reconstruction of an intact pelvis and femur

The 3D reconstruction of an intact pelvis and femur of a 27-year-old woman was carried out using X-ray computed tomographic (CT) images taken around the hip joint. Along the axial direction, 446 tomographic images were taken at intervals of 0.7 mm. Through the CT images, the sacrum, articular cartilages, left-side coxal bone, and cortical and cancellous bones of the femur were reconstructed using the commercial software, MIMICS of Materialise (see Figure 1(a)–1(f)).

For the articular cartilages, we reconstructed the gaps between the sacrum and the coxal bone and between the coxal bone and the femoral head in the CT images because an X-ray CT system cannot take images of soft tissues (see Figure 1(b) and 1(d)). The reconstructed, intact hip joint structure is shown in Figure 1(e).

2.2 Geometric solid modelling and Boolean operation as a virtual THA

The geometric solid modelling for each reconstructed model of the intact hip joint was performed using the

software, RapidForm of INUS Tech. Inc., Seoul, Korea. (see Figure 2(a)–2(e)). In order to reduce the difficulties in solid modelling, only one half of the sacrum was selected after considering the symmetric structure of the lower extremity. Also, the actual structure of the sacrum with sacral holes was simplified as a structure without holes (see Figure 2(a)).

For the fabrication of the geometric solid models of collarless and collared prostheses, CAD data of the PerFix collarless and collared prostheses of Japan Medical Materials Co., Ltd, Tokyo, Japan were used. The software, CATIA of Dassault Systems, Velizy-Villacoublay, France, was utilised to fabricate the solid models (see Figure 3(a)–3(e)). Considering the size of the patient's femur, the size of the stem and the length of the collar were modified from the standard CAD data of the PerFix prostheses using CATIA. The virtual THA, which includes a cutting process for the solid femoral head and a process for the insertion of solid collarless or collared prosthesis into the solid cancellous bone, was performed using Boolean operations.

The overall geometric solids of the intact hip joint and the hip joint after THA are shown in Figure 4(a) and 4(b).

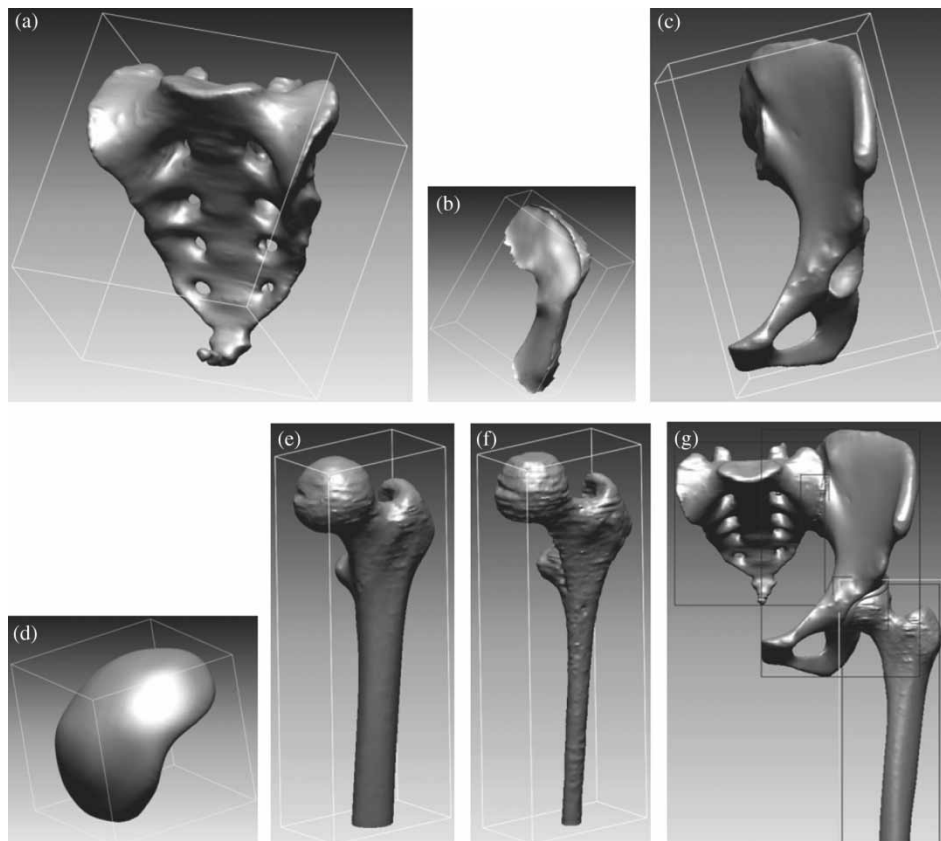


Figure 1. The reconstructed (a) sacrum, (b) articular cartilage (between the sacrum and the coxal bone), (c) left side coxal bone, (d) articular cartilage (between the coxal bone and the head), (e) cortical bone of the femur, (f) cancellous bone of the femur and (g) entire intact hip joint structure.

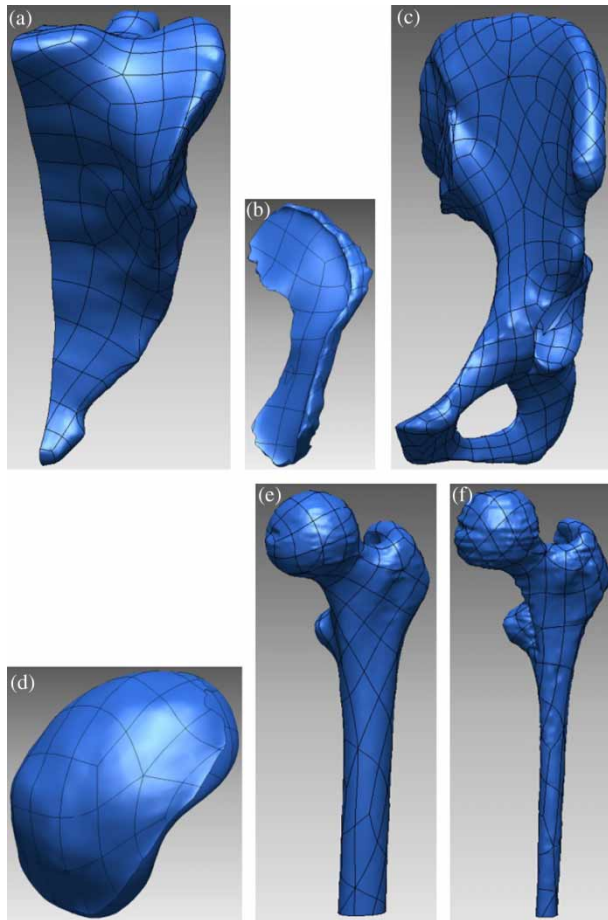


Figure 2. The geometric solid of (a) sacrum, (b) articular cartilage (between the sacrum and the coxal bone), (c) left side coxal bone, (d) articular cartilage (between the coxal bone and the head), (e) cortical bone of the femur and (f) cancellous bone of the femur.

The zoomed configurations around the proximal parts of the collarless and collared stems are shown in Figure 4(c) and 4(d). In this research, the state of perfect contact between the collar and the calcar is modelled to investigate the fundamental biomechanical functions of the collar (see Figure 4(d)).

2.3 Finite element modelling

Compatible 3D finite element meshes were generated directly in each solid model for the hip joints using the commercial software, PATRAN of MSC Software Corp., Santa Ana, USA. Figure 5(a)–5(d) shows the finite element models of the hip joints. For simplicity of modelling, the muscle sets around the hip joint were extremely simplified based on the muscle paths obtained from Visible Human Project (VHP, Bitsakos et al. 2005). Only four paths were selected to prevent the irrational

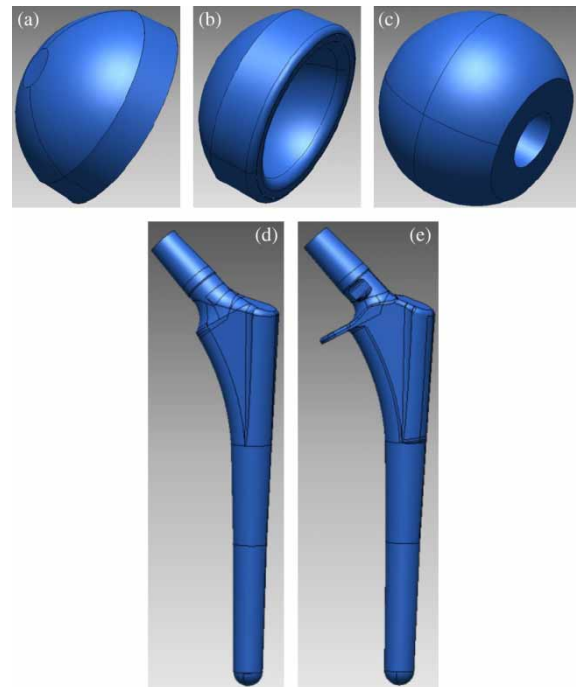


Figure 3. The geometric solid of (a) cup, (b) liner, (c) head, (d) collarless stem and (e) collared stem.

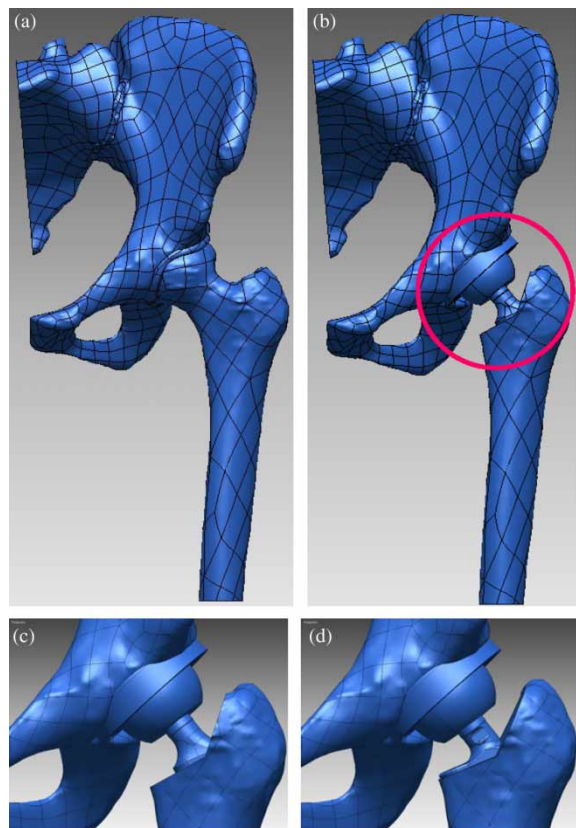


Figure 4. The entire geometric solid of (a) intact hip joint, (b) hip joint after THA, (c) zoomed configuration around collarless stem and (d) collared stem.

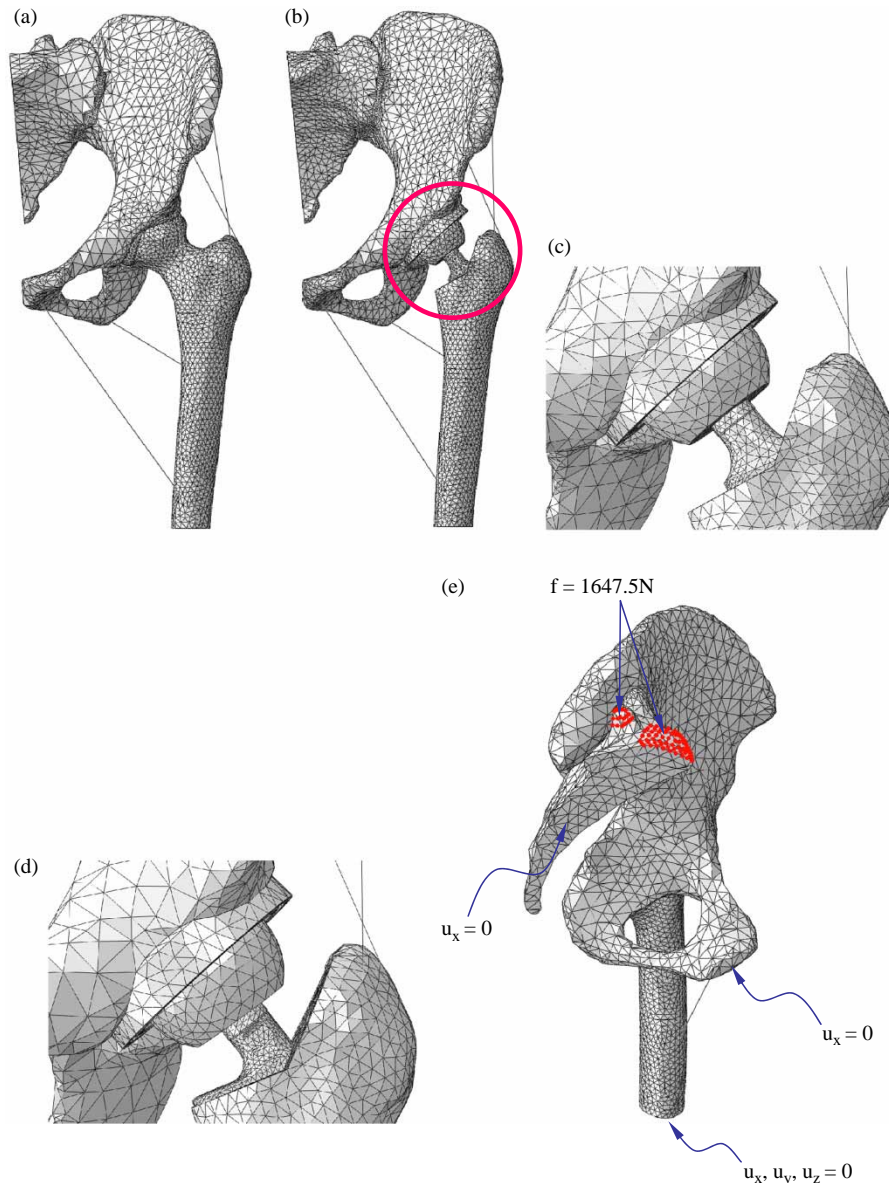


Figure 5. The entire finite element model of (a) intact hip joint, (b) hip joint after THA, (c) zoomed configuration around collarless, (d) collared stem and (e) the boundary condition for the computations.

deformation of the hip joint (see Figure 5(a) and 5(b)). Note that the same positions of attachment of the muscle paths to each finite element model of the coxal bone and femur were chosen carefully for obtaining consistent deformation behaviours of the hip joints.

Quadratic tetrahedral elements with 10 nodes were used for the overall models excepting the muscle paths for which linear truss elements with two nodes were used. In all, 113, 325 elements and 162, 403 nodes were used for the intact hip joint model. For the hip joint model that was implanted using a collarless stem, the respective elements and nodes were 115, 944 and 176,

024. For the hip joint model that was implanted using a collared stem, 116, 883 elements and 176, 610 nodes were used.

2.4 Material properties and boundary conditions

The relevant materials, such as the sacrum, the coxal bone, the cortical and cancellous bones of the femur, the articular cartilages, and the liner and the head of the prosthesis, were assumed to be isotropic and linear elastic. The materials for the cup and the stem were assumed to be isotropic and elastic-plastic with a power-law hardening

Table 1. The material properties used for the computations.

	Elastic modulus (GPa)	Poisson's ratio	Yield stress (MPa)
Cortical bone (Kopparti and Lewis 2007)	10.5	0.3	–
Cancellous bone (Kopparti and Lewis 2007)	0.15	0.2	–
Femoral/tibial articular cartilage (Li et al. 2001)	0.012	0.45	–
Stem (Ti-6Al-4V)	110	0.3	970
Cup (Ti-6Al-4V)	110	0.3	970
Head (Ceramic)	380	0.26	–
Liner (UHMWPE)	1.95	0.43	–

exponent of three (Jeon et al. 2009). In particular, a biocompatible material, viz., Ti alloy (Ti-6Al-4V), was selected for the cup and the stem. Table 1 shows the material properties of each component; these were used for the computations.

In terms of boundary conditions for the computations, the degrees of freedom in the x -, y -, and z -direction were constrained at the nodes on the distal end of the femur. At the nodes on the symmetric surfaces of the sacrum and coxal bones, a constraint was applied in the x -direction.

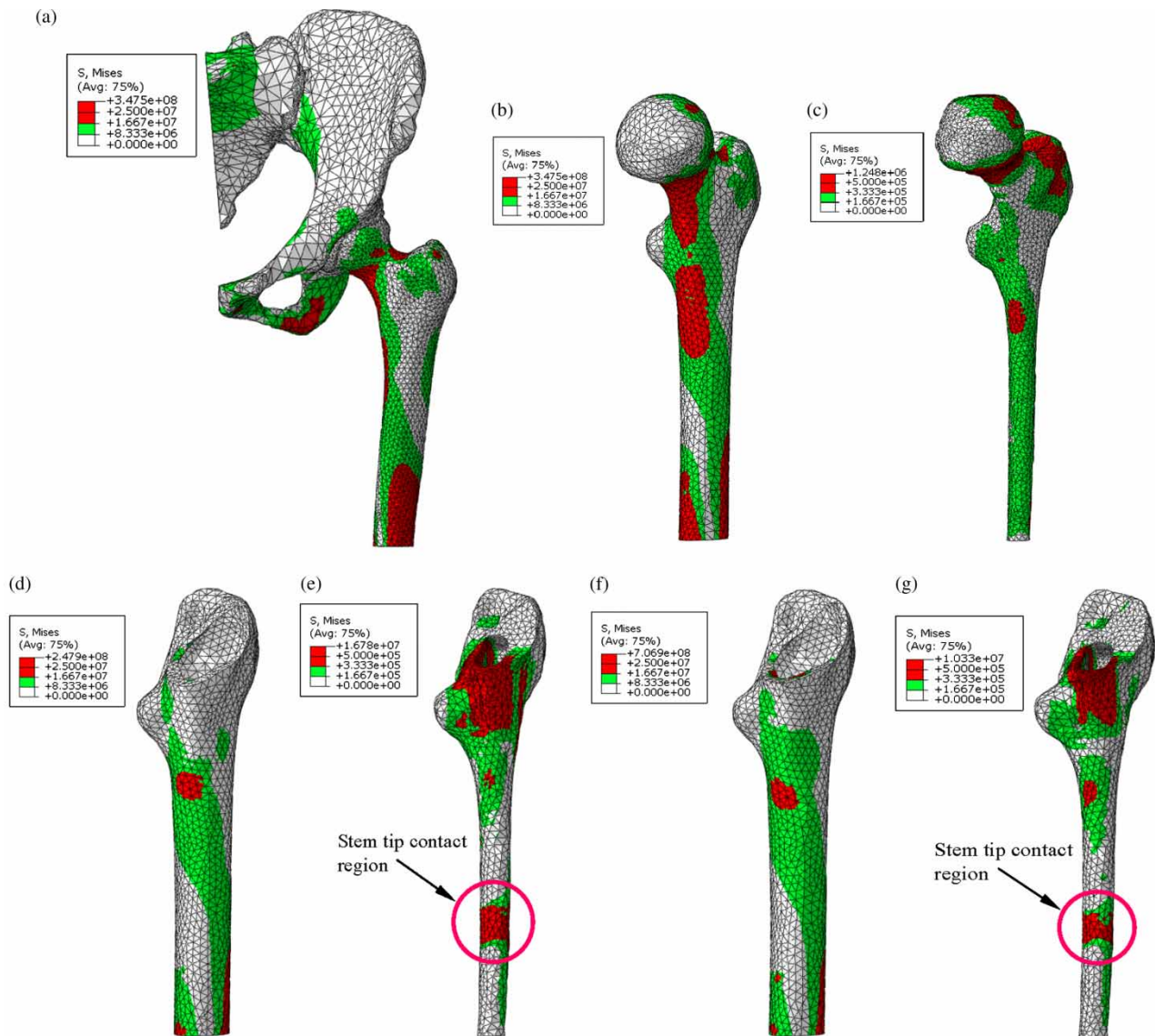


Figure 6. The von Mises stress distribution of (a) intact hip joint, (b) intact cortical, (c) cancellous bone, (d) implanted cortical bone, (e) cancellous bone using collarless stem, (f) implanted cortical bone and (g) cancellous bone using collared stem.

Downloaded By: [Bae, Ji Yong] At: 02:08 27 January 2011

On the base of sacrum and the facet of a sacral horn, three times of the woman's weight, viz., 1647.5N was applied; this load is transmitted through the L5 lumbar vertebrae and disc to the sacrum (see Figure 5(e)). The cup was assumed to be fixed perfectly on the coxal bone. Furthermore, the contact surfaces between the cup and the liner and between the head and the stem neck were tied perfectly with each other. The frictionless contact condition was applied between the articular cartilages of the coxal bone and the femoral head of the intact hip joint, and between the liner and the stem head. For modelling a cementless femoral stem, a frictional contact condition with a friction coefficient of 0.4, which was experimentally measured by Rancourt et al. (1990), was assumed for the contact surfaces between the stem and

the cancellous bone, and between the collar and the calcar.

3. Results and discussions

A software package, ABAQUS of Dassault Systems, was used for the computations. The obtained deformation shapes with the von Mises stress distributions of the intact hip joint are shown in Figure 6(a). Figure 6(b) and 6(c) shows the distributed von Mises stress in the intact cortical and cancellous bones. A high level of stress distribution is observed around the femoral neck. The distributed von Mises stress level in the cancellous bone is considerably smaller than that in the cortical bone because the hard cortical bone blocks the transmission of the applied load.

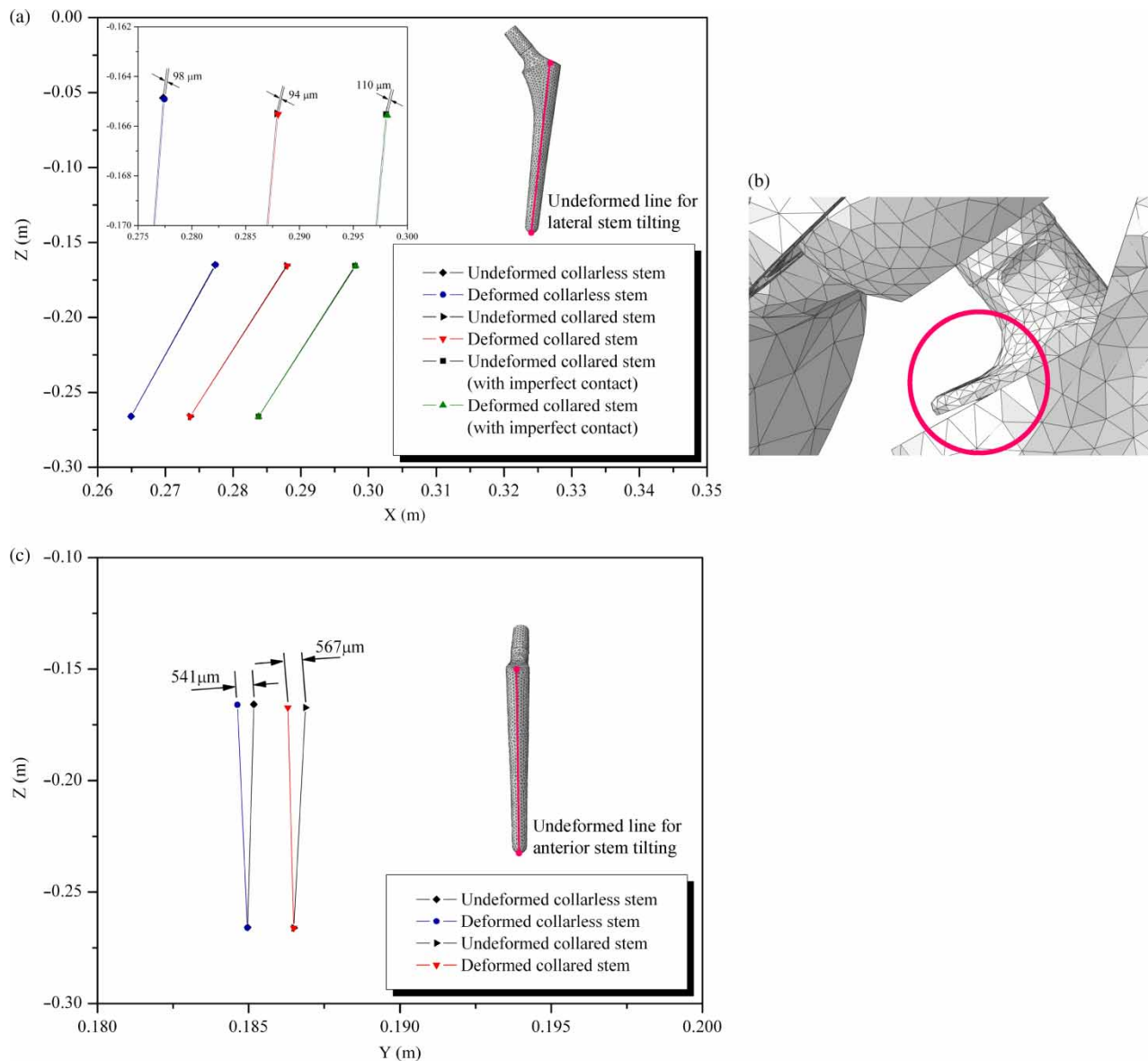


Figure 7. (a) The lateral stem tilting, (b) another model of a collared stem with imperfect calcar contact and (c) anterior stem tilting.

In the cancellous bone, the von Mises stress level on the neck portion is seen to be still higher than in other portions.

Figure 6(d) and 6(f) shows the von Mises stress distributions of the cortical bones after THA. This figure shows that the stress levels of the cortical bones after THA are considerably lower than those of the intact femur. In particular, the von Mises stress level around the calcar region of the cortical bones is significantly lower than that around the intact femoral neck region, even though a collared stem is used. This means that following THA, the stress shielding effect can occur in the cortical bone under

not only collarless but also collared stems; this effect causes calcar resorption after prolonged usage. However, the cortical bone that is implanted with a collared stem shows somewhat higher stress levels in the calcar region than those that are obtained under a collarless stem. Therefore, in terms of calcar resorption, a collared stem is somewhat more profitable than a collarless stem.

Figure 6(e) and 6(g) shows the distributed von Mises stress in the cancellous bones following THA. High stress levels are observed around the calcar regions of both cancellous bones, which result from direct contact with

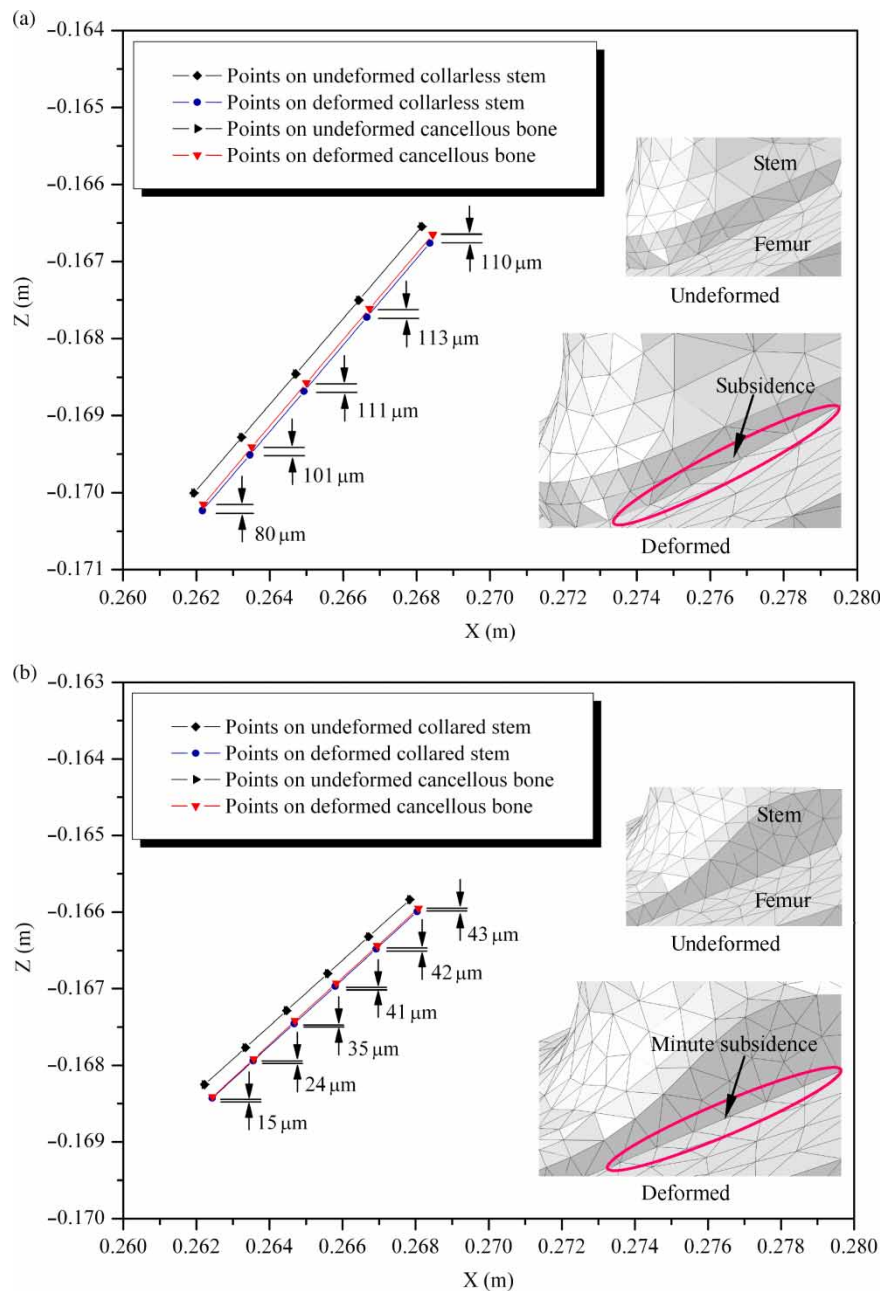


Figure 8. The subsidence of (a) collarless and (b) collared stems.

a stem of high stiffness. Considering the compressive strength of the cancellous bone, viz., 5 ~ 15MPa (Knaus 1981), local fracture is anticipated around the region, which can cause stem loosening and micromotion. Another region of concentrated stress is seen in the contact region between the stem tip and the cancellous bone. This concentration of stress suggests a high possibility of local bone fracture and can be regarded as a cause of mid-thigh pain (Namba et al. 1998). However, when a collared stem is used, we see that the concentrated von Mises stress level is lower than that obtained under a collarless stem. Therefore, a collared stem is more beneficial than a collarless stem for reducing the stress level on the cancellous bone.

The geometric tilting of the stem, which can be regarded as a significant cause of stem micromotion and loosening, is investigated. Figure 7(a) and 7(c) presents the lateral and anterior tilting of the stem, respectively. Two important facts are discerned from this figure. One is that the tilting of a collared stem is smaller than that of a collarless stem. This contrasts with the results of Fagan and Lee (1986), who report the greater tilting of a collared stem due to the role of the collar as a pivot. The reason for the smaller tilting of a collared stem in this present study is that the perfect contact between the collar and the calcar constrains the stem from tilting. To investigate in detail the phenomenon of lateral tilting for collared stems, another model of a collared stem with imperfect calcar contact is constructed and used for computation (see Figure 7(b)); the corresponding results are plotted in Figure 7(a). From the results, it is found that a collared stem with imperfect calcar contact causes the most severe tilting of the stem compared with other stems. In this case, the collar contacts gradually with the resected surface under applied loading; thereby the stem tilting is increased. Here, the collar can be seen as playing the role of a pivot.

Another observation is that the anterior tilting of the stem is also considerably large in comparison with the lateral tilting of the stem. This is due to the position of the applied load, which gives rise to a moment that causes femoral deformation in the anterior direction. As the collared stem in this research does not have projections in the anterior and posterior directions, the tilting of the collared stem is almost similar to that of a collarless stem. The subsidence of the stem into the femur and the proximal–lateral gap between the stem and the cancellous bone are observed. Figure 8(a) and 8(b) presents the subsidence of collarless and collared stems, respectively. Considerable subsidence is observed for the case of a collarless stem, whereas a collared stem causes only a little subsidence. Figure 9(a) and 9(b) shows the lateral gaps that are caused by collarless and collared stems. A collarless stem produces a larger lateral gap than a collared stem. Therefore, micromotion in the axial and lateral directions and loosening can be regarded as being easily caused by collarless stems.

From the results, we confirm that a collarless stem produces the stem subsidence, a large proximal–lateral gap, and large degrees of anterior and lateral tilting of the stem, which cause the stem micromotion in the axial and lateral directions and loosening, and can be the major

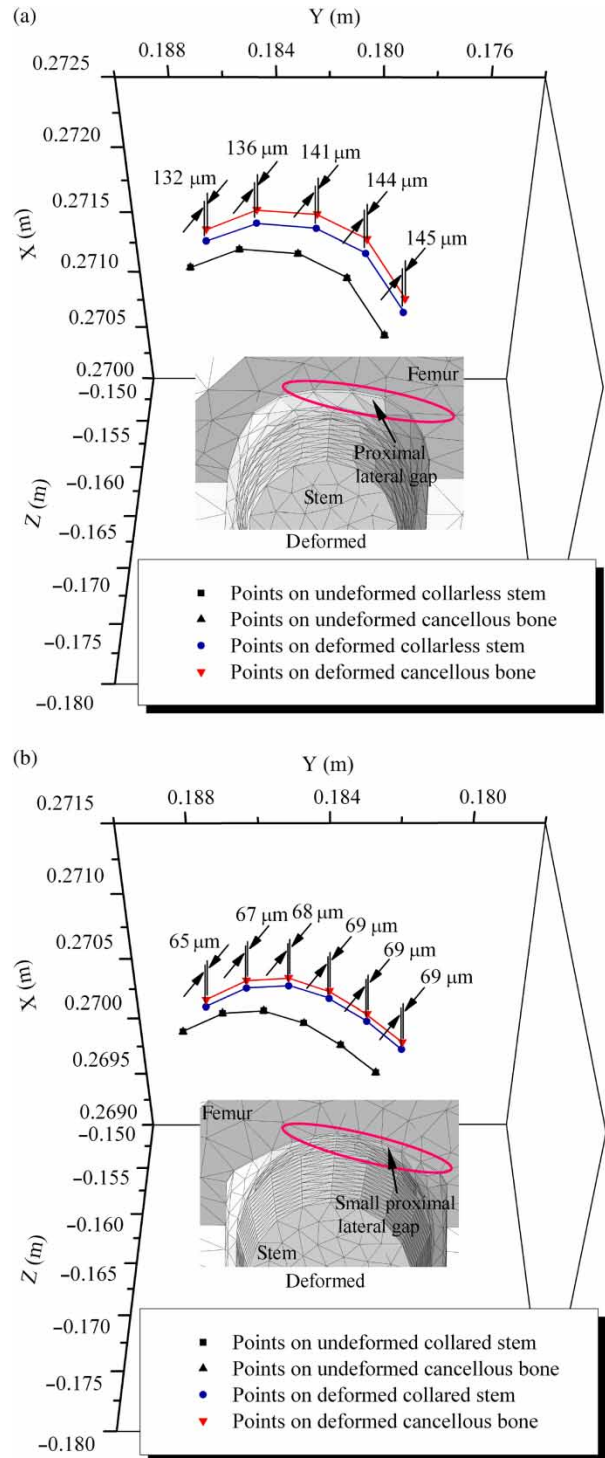


Figure 9. The proximal–lateral gap caused by (a) collarless and (b) collared stems.



Figure 10. The clinical results of a 70-year-old female patient (a) right after THA, (b) 2 weeks after THA, (c) 8 weeks after THA using a PerFix collarless stem; the clinical results of a 49-year-old female patient (d) right after THA, (e) 1 year after THA, (f) 8 years after THA using the a PerFix collared stem; a typical state of (g) varus deformation of hip joint and (h) the femoral fracture. ((g) and (h) sourced from <http://www.radiologyassistant.nl/en/431c8258e7ac3>).

causes of the femoral fracture. Figure 10(a)–10(c) shows the clinical follow-up results of a 70-year-old female patient after THA that used a PerFix collarless stem. In the figure, the stem subsidence is clearly observed after 2 weeks, and the femoral fracture is found after 8 weeks.

Moreover, we confirm that a collared stem with perfect calcar contact prevents stem subsidence and induces a small proximal–lateral gap, besides small degrees of anterior and lateral tilting of the stem. Therefore, it can impart proximal–stem fixation under a cyclic load that is applied over a long period of time. Figure 10(d)–10(f) shows the results of clinical follow-up for a 49-year-old female patient 8 years after THA that used a PerFix collared stem. From the figure, the biomechanical stability of a collared stem without any subsidence and femoral fracture is confirmed. However, there still exists a risk of calcar resorption because of the low ability of collared stems to transmit load. The zoomed image in Figure 10(f) clearly shows the resolved calcar shape. Also, a collared stem that contacts imperfectly with the calcar increases the lateral tilting of the stem. Therefore, depending on the status of calcar contact, and the size and shape of the stem, there exists a possibility of serious femoral fracture from the varus deformation of the hip joint (see Figure 10(g) and 10(h)).

4. Conclusions

In this research, the biomechanical effect of collars is analysed using computational and clinical follow-up results. A hip joint that was implanted using two cementless hip prostheses, one collared and the other collarless, and an intact hip joint are modelled and used for the computations. From the results, it is found that a collar that contacts perfectly with the calcar prevents stem subsidence and decreases the proximal–lateral gap between the cancellous bone and the stem, besides the lateral tilting of the stem. Therefore, a collar can impart reasonable biomechanical stability to the implanted stem.

However, there exists a risk of calcar resorption because of the low ability of the collar to transmit loads. Also, a collared stem with imperfect calcar contact increases the lateral tilting of the stem. As serious anterior tilting of the stem occurs during femoral deformation, both the lateral and the anterior tilting of the stem may bring about the varus deformation of the hip joint. Therefore, depending on the status of calcar contact, and the size and shape of the stem, a collared stem can cause femoral fracture, which is a serious problem to be solved.

Acknowledgements

This work was supported by Nuclear R&D Program through the National Research Foundation of Korea funded by the Ministry of Education, Science and Technology (2008-2006034).

Notes

1. Email: tryoon@chonnam.ac.kr
2. Email: todo@riam.kyushu-u.ac.jp

References

- Abdul Kadir MR, Kamsah N, Mohlisun N. 2008. Interface micromotion of cementless hip arthroplasty: collared vs. non-collared stems. Paper presented at: Biomed 2008. In proceedings of the 4th Kuala Lumpur International Conference on Biomedical Engineering; Kuala Lumpur, Malaysia.
- Bitsakos C, Kerner J, Fisher I, Amis AA. 2005. The effect of muscle loading on the simulation of bone remodeling in the proximal femur. *J Biomech.* 38:133–139.
- Carlsson AS, Rydberg J, Onnerfalt R. 1995. A large collar increases neck resorption in total hip replacement. *Acta Orthop.* 66:339–342.
- Eldridge DJ, Smith EJ, Hubble MJ, Whitehouse SL, Learmonth ID. 1997. Massive early subsidence following femoral impaction grafting. *J Arthroplasty.* 12:535–540.
- Fagan MJ, Lee AJC. 1986. Role of the collar on the femoral stem of cemented total hip replacements. *J Biomech Eng-T ASME.* 8:295–304.
- Goetzen N, Lampe F, Nassut R, Morlock MM. 2005. Load-shift numerical evaluation of a new design philosophy for uncemented hip prostheses. *J Biomech.* 38:595–604.
- Jeon I, Katou K, Sonoda T, Asahina T, Kang KJ. 2009. Cell wall mechanical properties of closed-cell Al foam. *Mech Mater.* 41:60–73.
- Kelly SS, Fitzgerald RH, Rand JA, Ilstrup DM. 1993. A prospective randomized study of a collar vs. a collarless femoral prosthesis. *Clin Orthop Relat Res.* 294:114–122.
- Knaus P. 1981. Material properties and strength behavior of spongy bone tissue at the coxal human femur. *Biomed Tech.* 26:200–210.
- Kopparti PS, Lewis G. 2007. Influence of three variables on the stresses in a 3D model of a proximal tibia-total knee implant construct. *Bio-Med Mater Eng.* 17:19–28.
- Kwong KSC. 1990. The biomechanical role of the collar of the femoral component of a hip replacement. *J Bone Joint Surg-Br.* 72:664–665.
- Li G, Lopez O, Rubash H. 2001. Variability of a three-dimensional finite element model constructed using magnetic resonance images of a knee for joint contact stress analysis. *J Biomech Eng.* 123:341–346.
- Loudon JR, Charnley J. 1980. Subsidence of the femoral prosthesis in total hip replacement in relation to the design of the stem. *J Bone Joint Surg-Br.* 62:450–453.
- Meding JB, Ritter MA, Keating EM, Faris PM, Edmondson K. 1999. A comparison of collared and collarless femoral components in primary cemented total hip arthroplasty. *J Arthroplasty.* 14:123–130.
- Namba RS, Kim AS, Skinner HB. 1998. Cementless implant composition and femoral stress. *Clin Orthop Relat Res.* 347:261–267.
- Rancourt D, Shirazi-Adl A, Drouin G, Paiement G. 1990. Friction properties of the interface between porous-surfaced metals and tibial cancellous bone. *J Biomed Mater Res.* 24:1503–1519.
- Whiteside LA, Amador D, Russel K. 1988. The effects of the collar on total hip femoral components subsidence. *Clin Orthop Relat Res.* 231:120–126.